EXPERIMENTAL INVESTIGATION OF AN IN-DUCT ORIFICE WITH BIAS FLOW UNDER MEDIUM AND HIGH LEVEL ACOUSTIC EXCITATION

Lin Zhou*[1],Hans Bodén[2]

[1]CCGEx, Competence Centre for IC-engine gas exchange
[2]Linné Flow Centre
MWL, Aeronautical and Vehicle Engineering, KTH
Teknikringen 8, 100 44 Stockholm, Sweden
* Corresponding author: linzhou@kth.se

This paper experimentally investigates the acoustic properties of an orifice with bias flow under medium and high sound level excitation. Orifices with two different edge configurations were tested.The study includes a wide range of bias flow velocities, various acoustic excitation levels and different frequencies. The nonlinear acoustic scattering matrix was identified by a finely controled two-source method. Acoustic properties, such as impedance, nonlinear scattering matrix and the eigenvalues were compared and discussed. Experimental results also show that bias flow makes the acoustic properties much more complex compared to the no bias flow case, especially when the velocity ratio between acoustic particle velocity and mean flow velocity is near unity.

1 Introduction

Orifice plates and perforates appear in many technical applications where they are exposed to high acoustic excitation levels and either grazing or bias flow or a combination. Examples are automotive mufflers and aircraft engine liners. Taken one by one the effect of high acoustic excitation levels, bias flow and grazing flow are reasonably well understood. The nonlinear effect of high level acoustic excitation has for instance been studied in Ref. [1–10]. It is well known from this literature that perforates can become non-linear at fairly low acoustic excitation levels. The non-linear losses are associated with vortex shedding at the outlet side of the orifice or perforate openings [9, 10]. The effect of bias flow has for instance been studied in Ref. [11–17]. Losses are significantly increased in the presence of bias flow, since it sweeps away the shed vortices and transforms the kinetic energy into heat, without further interaction with the acoustic field. The combination of bias flow and high level acoustic excitation has been discussed and studied in Ref. [18] and some experimental investigations have been made in Ref. [19]. Luong [18] derived a simple Rayleigh conductivity model for cases when bias flow dominates and no flow reversal occurs. However, bias flow does not always play a positive role for sound dissipation of the orifice. Especially for orifices with some thickness, the whilslting potentiality brings the risk for additional sound production in the orifice. In Ref. [20], the whistling potential was studied in terms of the eigenvalues of the two-port matrix for the orifice.

The purpose of the present paper is to make a detailed study of the transition between the case when high level nonlinear acoustic excitation is the factor determining the acoustic properties to the case when bias flow is most important. As discussed in Ref. [18], it can from a theoretical perspective be expected that this is related to if high level acoustic excitation causes flow reversal in the orifice or if the bias flow maintains the flow direction, which is illustrated as Region 1 to Region 3 shown in Fig.1.

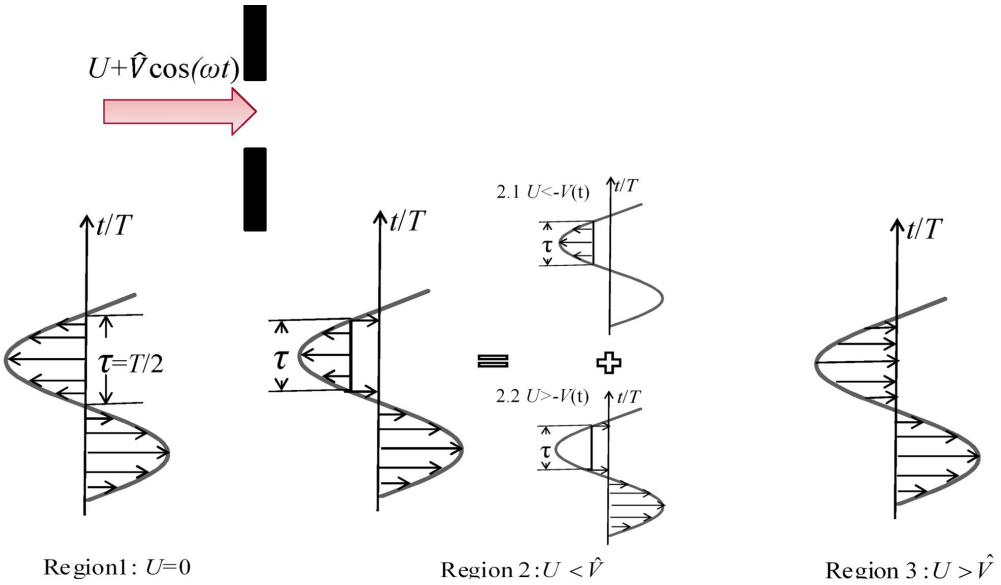

Figure 1: Flow directions through the orifice for different regions.

In the first section, the finely controlled two source method is introduced for the nonlinear scattering matrix identification based on the assumption that the acoustic nonlinearity is only related to the amplitude of acoustic pressure difference. The eigenvalues of scattering matrix is derived from impedance for low frequency. In the second section, the impedance of two orifices with different configuration is measured and discussed. The nonlinear acoustic matrix and its eigenvalues are investigated to study the potentiality of acoustic energy dissipation or production.

2 Theoretical background

Consider a small orifice installed between two uniform pipe segments. Low porosity gives relative high acoustic flow velocity in the orifice while it is much lower in the pipe where it is assumed that linear acoustic propagation applies. It is also assumed, supported by experimental evidence, that nonlinear propagation effects can be neglected. This makes it possible to use the two-microphone wave decomposition method to identify the wave components on both sides of the orifice as shown in Fig.2.

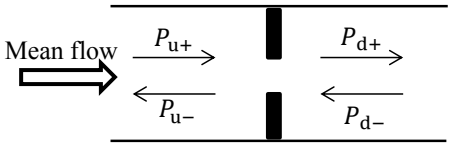

Figure 2: Forward and backward travelling wave components.

$$\begin{bmatrix} e^{-ik_+ d_i} & e^{ik_- d_i} \\ e^{-jk_+ d_j} & e^{jk_- d_j} \end{bmatrix} \begin{bmatrix} P_+ \\ P_- \end{bmatrix} = \begin{bmatrix} P_i \\ P_j \end{bmatrix}, \tag{1}$$

where $k_\pm$ are the wavenumbers for forward and backward planar waves. Following a model proposed by Dokumaci [21], the effect of viscos-thermal damping in pipe was included as

$$k_{\pm} = \frac{\omega}{c_0}\frac{K_0}{1 \pm K_0 M}, \tag{2}$$

where

$$K_0 = 1 + (\frac{1-\mathrm{i}}{s\sqrt{2}})(1 + \frac{\gamma - 1}{\sqrt{\mathrm{Pr}}}), \tag{3}$$

where $s = R\sqrt{\omega/\nu}$ is the shear wavenumber; R is the duct radius; γ is the ratio of specific heats and Pr is the Prandtl number; M is mean flow Mach number in the pipe.

With the planar wave components ($P_{\mathrm{u}+}$,$P_{\mathrm{u}-}$,$P_{\mathrm{d}+}$,$P_{\mathrm{d}-}$) on both sides, the oscillating velocity $\hat{V}$ in the orifice and acoustic properties, such as the normalized impedance can be given as

$$\hat{V} = \frac{P_{\mathrm{u}+} - P_{\mathrm{u}-}}{\rho_0 c_0 \sigma}, \tag{4}$$

$$Z = \frac{P_{\mathrm{u}+} + P_{\mathrm{u}-} - P_{\mathrm{d}+} - P_{\mathrm{d}-}}{\rho_0 c_0 \hat{V}}, \tag{5}$$

where $\sigma = (r/R)^2$, r is the radius of orifice hole.

2.1 Nonlinear scattering matrix identification

In order to reach acoustic nonlinearity in the presence of mean flow, the acoustic flow velocity should be of the same order of magnitude as the mean flow velocity. Both Mach numbers for mean flow and acoustic flow is much less than unity in the main pipe. Therefore, both the nonlinear acoustic energy flux and the part involving mean flow can be neglected, wich gives the approximation for energy flux in the pipe as,

$$I = (1 + M^2) < pv > + M[(< p^2 > /(\rho_0 c_0)) + \rho_0 c_0 < v^2 >] \approx < pv >, \tag{6}$$

which is the same as for linear acoustic propagation in the pipe without mean flow. What in Ref. [22] is denoted the energy scattering matrix of an orifice, which using the assumption that mean flow effects can be neglected in the main pipe is the same as the ordinary scattering matrix, can be expressed as

$$\begin{bmatrix} P_{\mathrm{u}-} \\ P_{\mathrm{d}+} \end{bmatrix} = \mathbf{S} \begin{bmatrix} P_{\mathrm{u}+} \\ P_{\mathrm{d}-} \end{bmatrix}. \tag{7}$$

The nonlinear energy scattering matrix **S** has four elements and to identify them we need two sets of different acoustic load cases. In the framework of small perturbation, which belongs to linear scattering matrix identification, either two-load or two-source methods can be used with any low level acoustic excitation for the identification. However, in the region of high acoustic excitation the scattering matrix vary with the level of acoustic excitation. A reasonable assumption could be that the nonlinearity of the scattering matrix is only based on the acoustic pressure difference over the orifice or the acoustic velocity in the orifice, but not individually depended on the acoustic pressure on each side. This assumption makes it possible to use either the two-load or two-source method for the identification. The additional condition which should be added is to keep the same magnitude of acoustic pressure difference or the same magnitude of acoustic flow velocity in the orifice. It can be expressed as

$$\begin{bmatrix} P^{\mathrm{I}}_{\mathrm{u}-} & P^{\mathrm{II}}_{\mathrm{u}-} \\ P^{\mathrm{I}}_{\mathrm{d}+} & P^{\mathrm{II}}_{\mathrm{d}+} \end{bmatrix} = \mathbf{S} \begin{bmatrix} P^{\mathrm{I}}_{\mathrm{u}+} & P^{\mathrm{II}}_{\mathrm{u}+} \\ P^{\mathrm{I}}_{\mathrm{d}-} & P^{\mathrm{II}}_{\mathrm{d}-} \end{bmatrix}, \tag{8}$$

$$|P^{\mathrm{I}}_{\mathrm{u}} - P^{\mathrm{I}}_{\mathrm{d}}| = |P^{\mathrm{II}}_{\mathrm{u}} - P^{\mathrm{II}}_{\mathrm{d}}|, \tag{9}$$

where $P^{\mathrm{I,II}}_{\mathrm{u}} = P^{\mathrm{I,II}}_{\mathrm{u}+} + P^{\mathrm{I,II}}_{\mathrm{u}-}$,and $P^{\mathrm{I,II}}_{\mathrm{d}} = P^{\mathrm{I,II}}_{\mathrm{d}+} + P^{\mathrm{I,II}}_{\mathrm{d}-}$.

2.2 Eigenvalues of $\mathbf{I}-\mathbf{S}^*\mathbf{S}$ for low frequency

In the presence of mean flow, the eigenvalues of the energy scattering matrix are indicators for the potentiality of acoustic dissipation or generation [22]. For low frequencies the thickness of the orifice is quite small compared with the wavelength and one can assume that the acoustic velocity is the same on both sides. In addition to eqn (5), one can get

$$\begin{bmatrix} P_u \\ \hat{V}_u \end{bmatrix} = \begin{bmatrix} 1 & \rho_0 c_0 Z \\ 0 & 1 \end{bmatrix} \begin{bmatrix} P_d \\ \hat{V}_d \end{bmatrix}, \tag{10}$$

where $\hat{V}_\mathrm{u} = (P_{\mathrm{u}+} - P_{\mathrm{u}-})/(\rho_0 c_0 \sigma)$,and $\hat{V}_\mathrm{d} = (P_{\mathrm{d}+} - P_{\mathrm{d}-})/(\rho_0 c_0 \sigma)$. With eqn (7) the energy scattering matrix can be expressed as

$$\mathbf{S} = \frac{1}{2+Z/\sigma} \begin{bmatrix} Z/\sigma & 2 \\ 2 & Z/\sigma \end{bmatrix}. \tag{11}$$

So the eigenvalues of $\mathbf{I}-\mathbf{S}^*\mathbf{S}$ is

$$\lambda_1 = 0, \lambda_2 = \frac{4(Z^*+Z)/\sigma}{(2+Z/\sigma)^*(2+Z/\sigma)}. \tag{12}$$

which means that for the resistance Re(Z)>0, there is a positive eigenvalue and the acoustic energy is dissipated, while for Re(Z)<0, the eigenvalue is negative and the acoustic energy is generated.

3 Experimental setup

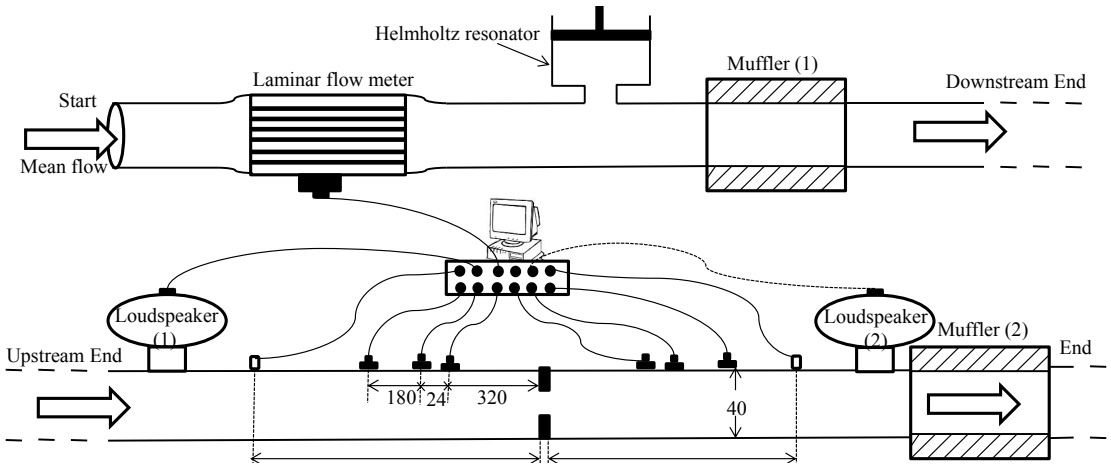

Figure 3: Schematic of the experimental setup, dimensions in millimetres.

The experimental setup is illustrated in Fig.3. The test object is an orifice plate mounted in a duct with a diameter of 40 mm. Six microphones were divided into two groups and symmetrically installed on both sides of the test sample so that the two-microphone wave ecomposition method could be used to identify the sound wave components on each side. Two different transducer separations (24mm and 180mm) gave a frequency arrange from 80Hz up to 5000Hz. On both sides, a high quality loudspeaker was mounted as the excitation source. For most acoustic impedance identifications, only the loudspeaker on the upstream side was used, while both were used for the nonlinear scattering matrix identification. The acoustic excitation levels were finely controlled so the amplitude of oscillating velocity in the orifice could be kept constant. Pure tone acoustic excitation was used and we made sure that nonlinear harmonics were sufficiently small when performing high pressure measurement. In order to

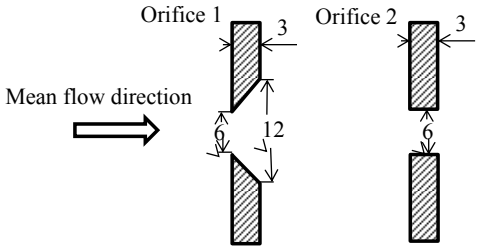

Figure 4: Orifice geometry, Orifice1: chamfer-edged, Orifice 2: thick sharp-edged.

measure the mean flow velocity, on the upstream side, a laminar flow meter was employed during the experiment. A sound attenuation system, including a tunable Helmholtz resonator and a muffler, was designed to attenuate the sound to less than 126 dB at the position of the laminar flow meter, to reduce the measurement error caused by the fluctuating flow. During the experiment the steady pressure drop over the orifice was also monitored by two pressure sensors installed further away from the test sample than the microphones. The mean flow discharge coefficient could be calculated as

$$C_{\mathrm{cM}} = \frac{U}{\sqrt{2\Delta P/\rho_0}}. \tag{13}$$

In the study, a wide range of mean flow (0-19m/s in the orifice), sound levels (100-155dB) and frequencies (100-1000Hz) were considered. Two orifice plates were tested, which have the same thickness and hole diameter, but different edges, as shown in Fig.4. Orifice1 does not have a perfect sharp edge on the upstream side. Instead it has an equivalent thickness about 0.6mm for the hole with diameter of 6mm.

4 Results and discussion

4.1 Acoustic impedance without bias flow

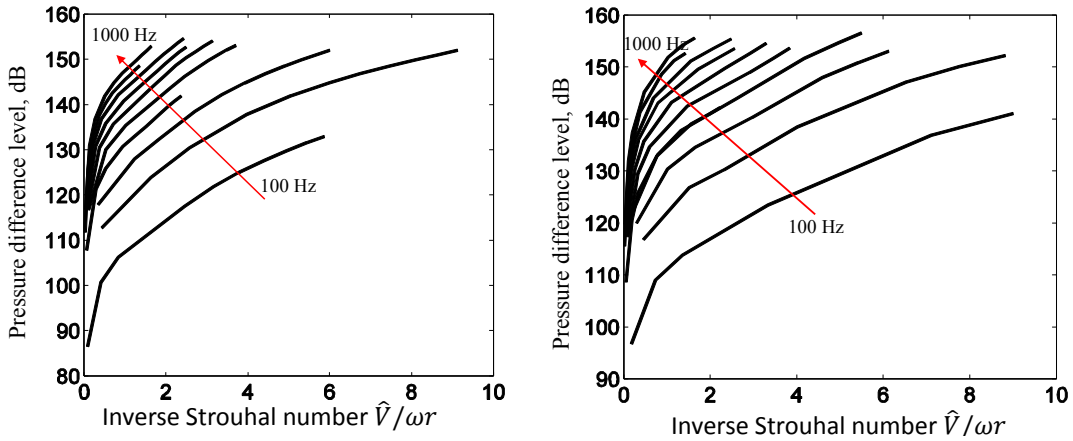

Figure 5: Pressure difference level plotted against inverse Strouhal number ($\hat{V}/\omega r$), frequency range: 100-1000Hz, (a): Orifice 1, (b): Orifice 2.

A wide range of frequencies and acoustic excitation have been studied in the test campaign. The range of frequency is from 100Hz to 1000Hz with a step of 100Hz. As show in Fig.5, the pressure difference is from below 120dB up to about 155dB plotted as a function of acoustic inverse Strouhal number. Fig.6 shows the normalized impedance divided by the Helmholtz number, which makes the curves for different frequencies collapse. There is a fairly good agreement between experimental resistance and

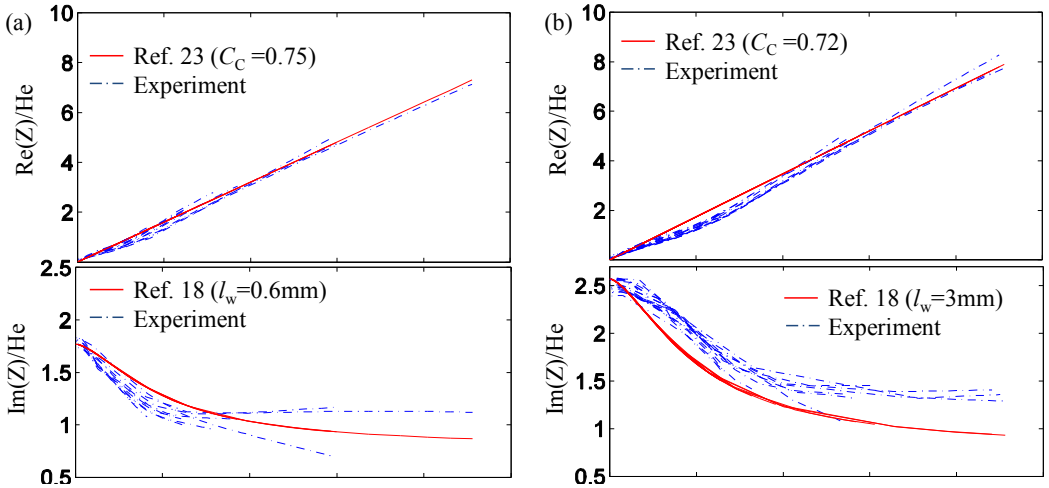

Figure 6: Normalized acoustic impedance divided by Helmhotz number ($\omega r/c_0$) plotted against inverse Strouhal number ($\hat{V}/\omega r$), frequency range: 100-1000Hz, (a): Orifice 1, (b): Orifice 2.

the analytical results which is from the resistance model eqn (24) in Ref. [23] with discharge coefficient 0.75 for Orifice 1 and 0.72 for Orifice 2.

For the reactance the analytical results, which is following the empirical Cummings effective length model as eqn (3.5) in Ref. [18]. have a qualitative consistence with our experimental results as shown in Fig.6. The experimental results show that the reactance have a constant value with an effective length $l = l_w + 2l_0$ (l_w is orifice thickness, and $l_0 = (\pi/4)r$ is the one-side end correction as in Ref.18) at low acoustic levels; decrease with higher acoustic excitation levels; and tend to a constant level with a small value at high excitation levels. This minimum reactance value seems to vary with different orifice geometries. Compared with the thick orifice (Orifice 2) the reactance for the thin orifice (Orifice 1) is much more sensitive to the acoustic excitation.

4.2 Acoustic impedance with bias flow

Table 1: Measured bias flow velocity and mean flow discharge coefficient

Orifice1			Orifice2		
Bias flow velocity U(m/s)	Reynolds number $2Ur/\nu$	Discharge coefficient C_{cM}	Bias flow velocity U(m/s)	Reynolds number $2Ur/\nu$	Discharge coefficient C_{cM}
2.8	1084	0.663	3.9	1510	0.799
7.8	3019	0.676	7.4	2865	0.610
11.5	4452	0.697	11.7	4529	0.687
			14.5	5613	0.645
			18.6	7200	0.684

In the presence of bias flow the acoustic properties becomes quite complicated, since it is not only a function of acoustic excitation level and frequency but also influenced by mean flow velocity. In view of the flow pattern, both bias flow and acoustic flow can be laminar or turbulent depending on their Reynolds numbers. Table 1 provides parameters for the bias flow in two orifices used in the experiments. The mean flow discharge coefficient is calculated according to eqn (13). In most cases the values are between 0.6 and 0.7 which are typical for turbulent flow in orifices. The exception is the case with low Reynolds number for Orifice 2 where the discharge coefficient is around 0.8.

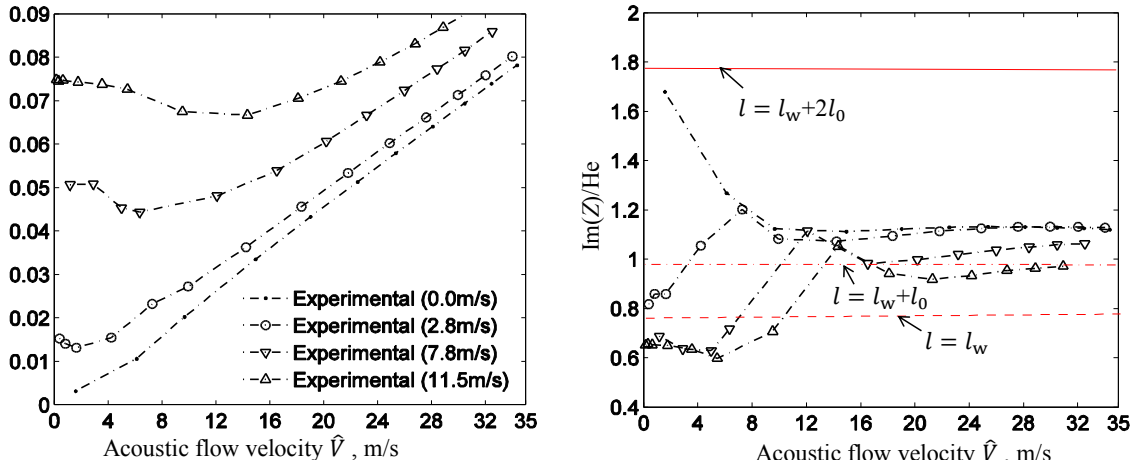

Figure 7: Normalized acoustic impedance for different bias flow velocities, Orifice 1, frequency: 200Hz.

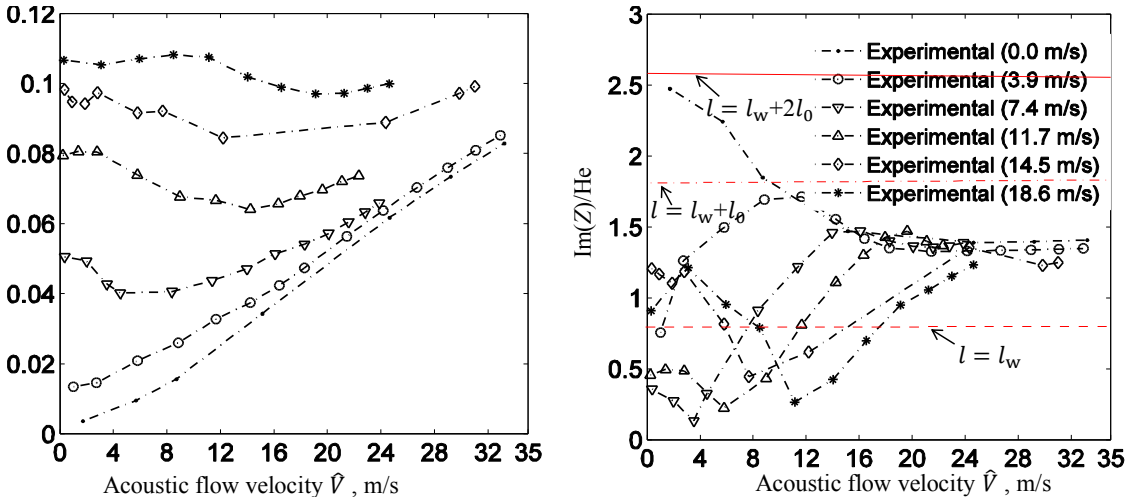

Figure 8: Normalized acoustic impedance for different bias flow velocities, Orifice 2, frequency: 200Hz.

Fig.7 and Fig.8 compare acoustic impedance results for the two orifices with different bias flow velocities and low to high acoustic excitation levels, which is from Region 3 ($U > \hat{V}$) to Region1($U = 0$ or $U << \hat{V}$). The results show that the acoustic resistance firstly decreases with an increase in acoustic excitation level, and then tend to increase and approach the result without bias flow. The minimum is obtained when the acoustic velocity is similar in magnitude to the bias flow velocity. The reason could be related to the difference in values of mean flow discharge and acoustic discharge coefficient, otherwise the risistance should increase at the beginning according to Cummings equation [6, 18].The reactance, which is plotted divided by the Helmholtz number, has varying values for low acoustic excitation depending on mean flow velocity and orifice geometries. The values are even smaller than the one-sided end correction for relative high bias flow levels. Compared with the no bias flow case, even a very small bias flow can decrease the reactance substantially for low acoustic excitation levels. With increase of acoustic excitation, the acoustic reactance starts to increase to a maximum value. Then it behaves similar to that in the no bias flow cases. This transfer point for acoustic flow velocity depends on the bias flow velocity. The higher the bias flow velocity, the higher acoustic excitation it needs.

Acoustic impedance is also frequency dependent as illustrated in Fig.9 and Fig.10 where the values of acoustic impedance for different frequencies with the same bias flow velocity for both orifices are

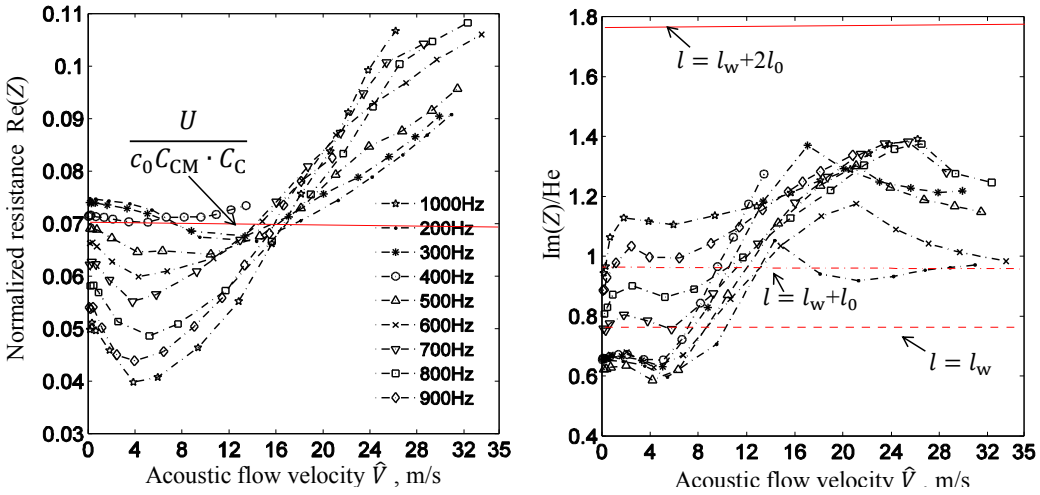

Figure 9: Normalized acoustic impedance for different frequencies, Orifice 1, U=11.5 m/s.

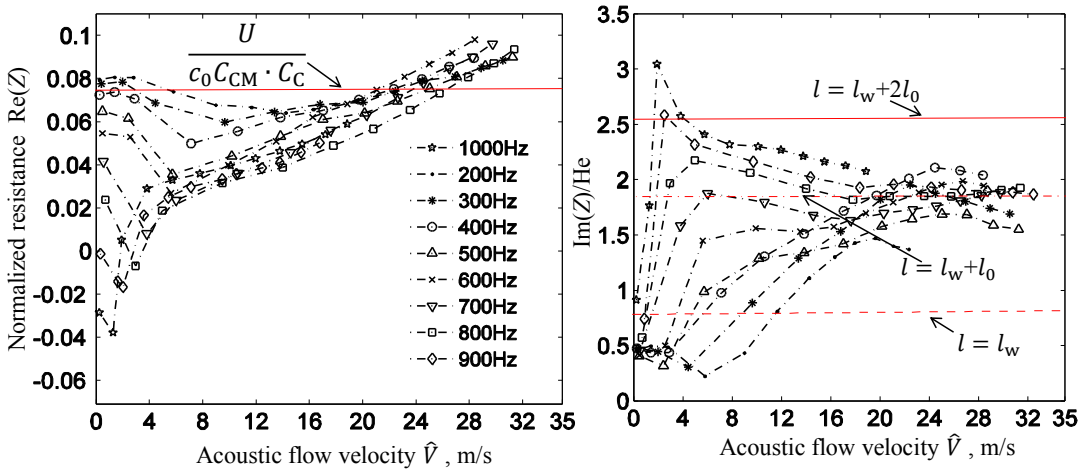

Figure 10: Normalized acoustic impedance for different frequencies, Orifice 2, U=11.7 m/s.

shown. For Region 3 ($U > \hat{V}$), low frequencies and low acoustic excitation, the value for resistance is quite close to the analytical result, which is $U/(c_0 C_{CM} C_C)$ according to Cummings equation. In this case, the flow jet kinetic energy changes slowly. So the flow discharge coefficient (C_C) should be quite stable and close to the value in the absence of acoustic excitation($C_C = C_{CM}$), which was measured and used for the analytical model. For higher frequencies the dimension of unsteady vorticity out of the imcompressible jet should be in the order of magnitude $\sim U/\omega$, which means that the scale of turbulence decreases with increasing frequency. Therefore additional irrotational flow is developed and the flow discharge coefficient increase with the vena contracta area expansion. As stated in Ref. [18], this irrotational response in exterior fluid must become essentially similar to that in the absence of the jet (bias flow).So higher frequencies decrease the acoustic resistance and increase the acoustic reactance, as shown in Fig.9. Comparing the thick orifice (Orifice 2) to the thin (Orifice 1), the resistance for some high frequencies even decreased to a negative value and the reactance sharply increased at low acoustic excitation. The reason is that these frequencies (800-1000Hz) fall into the arrange of flow instability, where the Strouhal number based on orifice thickness and bias flow ($f l_w/U$) equals 0.2-0.35 [20]. Even though increasing acoustic excitation increases the resistance to positive values. This means that high acoustic levels seem to drcrease the flow instability.

4.3 Nonlinear acoustical energy disppation/production

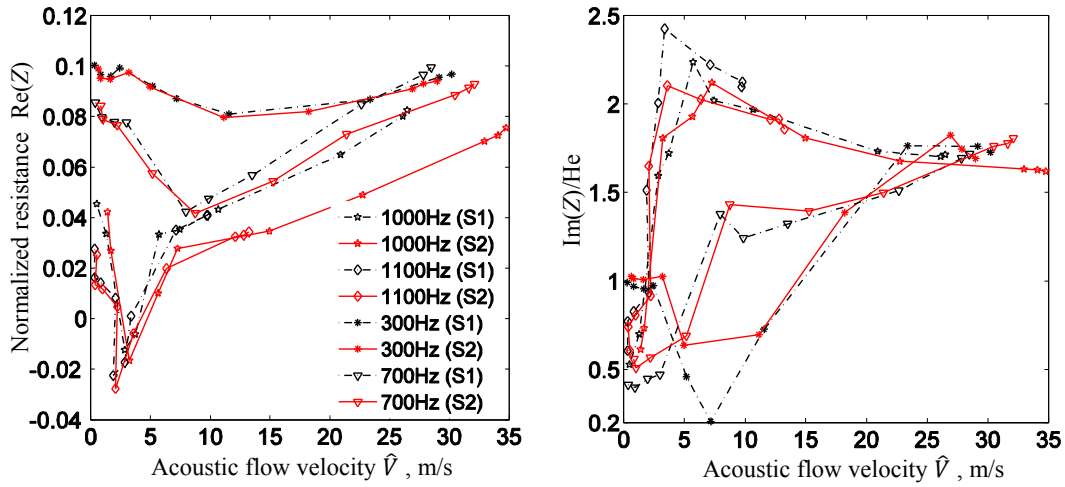

Figure 11: Normalized acoustic impedance for different acoustic excitation position, Orifice 2, U=14.5 m/s.

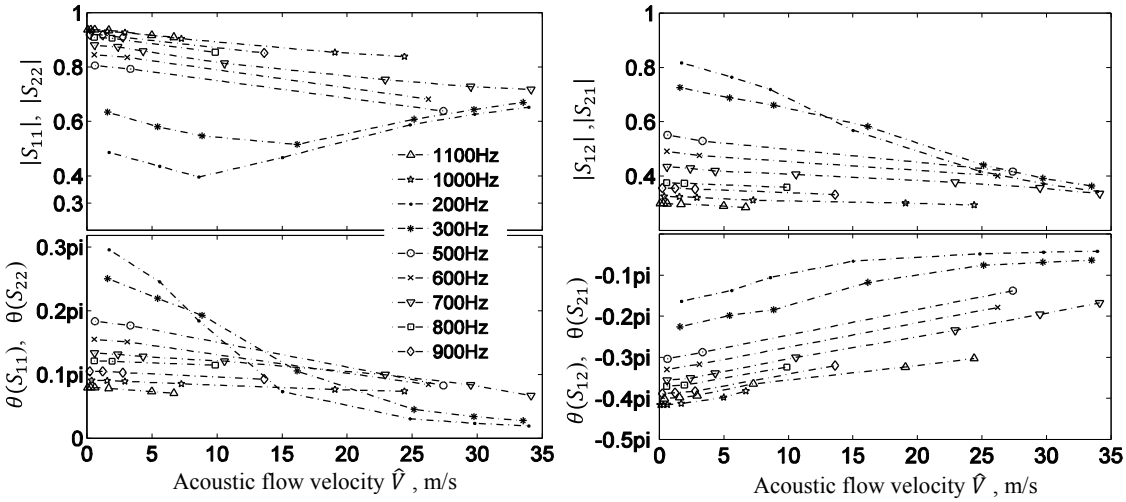

Figure 12: Scattering matrix without bias flow, Orifice 2.

The scattering matrix is a full map of acoustic properties of an sample. For linear scattering matrix the acoustic properties are assumed to be independent of the acoustic excitation level. Here it is assumed that the elements of the scattering matrix can vary the amplitude of pressure difference or the acoustic flow in the orifice. The varying acoustic excitation was obtained by loudspeaker excitation on the upstream side (S1) and downstream side (S2). Some results are shown in Fig.11. For high level excitation under high frequencies, there is some difference for the resistance. It could be related to interaction from the acoustic field with the asymmetrical out-orifice turbulence flow.

The nonlinear scattering matrix is quite symmetrical as previous discussion and the measured results are shown in Fig.12 for the cases without bias flow and in Fig. 13 for the cases with bias flow. For the no bias flow cases, both the reflection (S11,S22) and transmission(S12, S21) decreases with increasing levels of acoustic excitation as well as increasing frequency. The exception is only for the resistance for high acoustic levels with high frequencies. For the cases with bias flow the reflection increases sharply in the

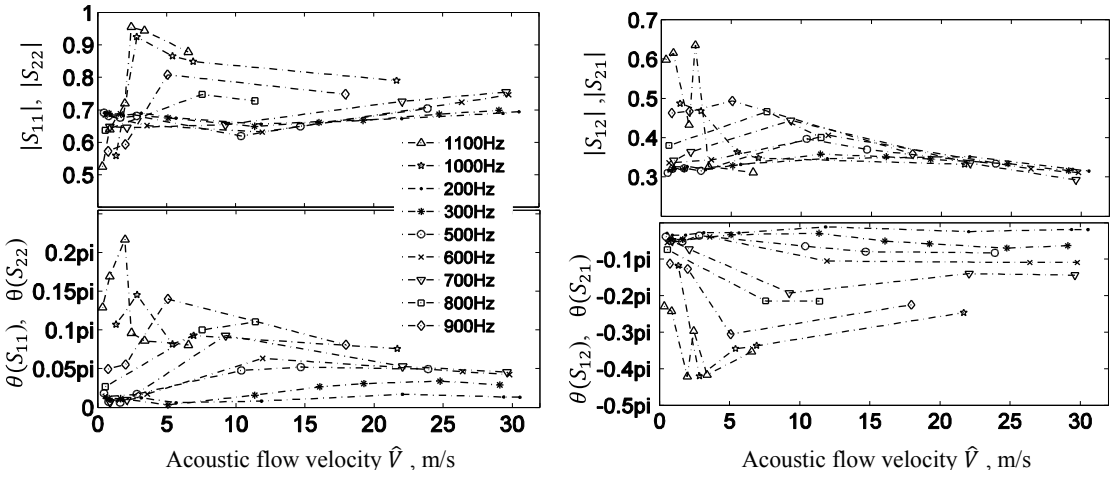

Figure 13: Scattering matrix with bias flow, Orifice 2, U=14.5 m/s.

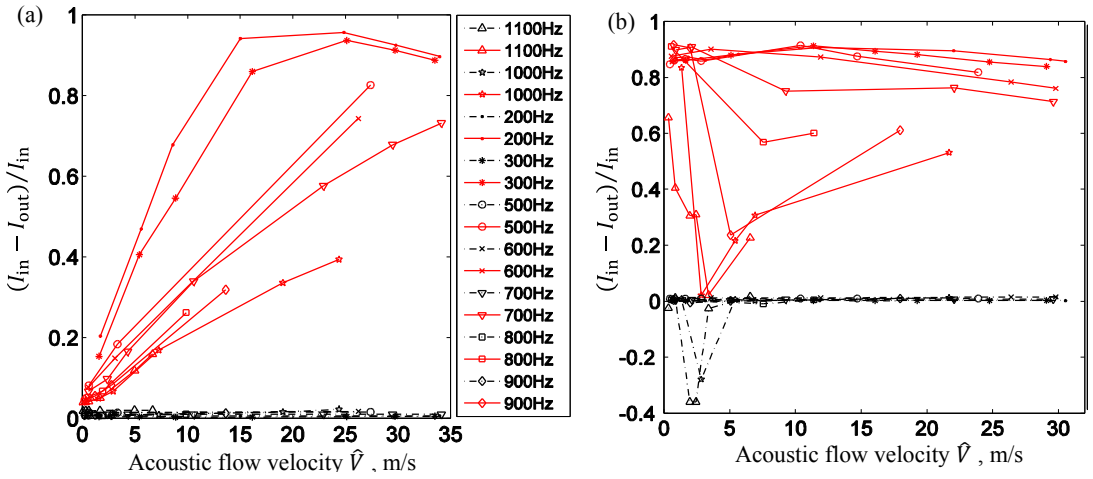

Figure 14: Eigenvalues representing the ratio of dissipated acoustic power, Orifice 2, (a): U=0 m/s, (b): U=14.5 m/s.

unstable acoustic excitation level region, where the eigenvalues of are negative as shown in Fig.14. The high level acoustic excitation increases the acoustic energy dissipation especially for low frequencies as shown in Fig.14(a). Fig. 14(b) shows that for the frequencies far from flow instability bias flow can also greatly increase the dissipation for low and medium acoustic excitation. The unstable flow region, where the eigenvalues tend to be negative coincides with the region of negative resistance as shown in Fig. 11. This means that for thin orifices and low frequencies the resistance could be an alternative indication for the prediction of flow instability. It also seems that higher level acoustic excitation can influence the flow pattern and bring back the flow to a stable level.

5 Conclusions

In this paper, the nonlinear acoustic properties of orifices under high acoustic excitation and with bias flow have been studied for different frequencies. It was seen that without bias flow the acoustic impedance only dependends on the inverse acoustic Strouhal number and there is a reasonably good agreement between analytical model results and measurements for the acoustic resistance. The reactance model based on Cummings effective length model catches the initial decrease with increasing

excitation but has larger errors for high excitation levels. For the case with bias flow, when acoustic excitation is low, the resistance decrease with frequency, while the reactance increases. Orifice thickness influences the flow stability and the resistance tends to be negative while the reactance increases sharply with a relative small increase of acoustic excitation level for a specific range of flow Strouhal numbers. For medium acoustic excitation levels, both resistance and reactance increase with the acoustic excitation. A minimum frequency dependent value exists for resistance when the acoustic flow velocity is of the same magnitude or slightly smaller than the bias flow velocity. For high acoustic excitation the acoustic impedance is similar to that for the no bias flow case. The acoustic energy dissipation potentiality can be increased either by high level acoustic excitation, or by the bias flow for low and medium acoustic excitation and frequencies far from the unstable region. Experimental results also show that high level acoustic excitation can influence the flow stability.

References

[1] L. J. Sivian. Acoustic impedance of small orifices. *Journal of the Acoustical Society of America*, 7:94–101, 1935.

[2] U. Ingård and S. Labate. Acoustic circulation effects and the nonlinear impedance of orifices. *Journal of the Acoustical Society of America*, 22:211–219, 1950.

[3] U. Ingård and H. Ising. Acoustic nonlinearity of an orifice. *Journal of the Acoustical Society of America*, 42:6–17, 1967.

[4] T.H. Melling. The acoustic impendance of perforates at medium and high sound pressure levels. *Journal of Sound and Vibration*, 29(1):1 – 65, 1973.

[5] B.T. Zinn. A theoretical study of non-linear damping by helmholtz resonators. *Journal of Sound and Vibration*, 13(3):347 – 356, 1970.

[6] A. Cummings. Transient and multiple frequency sound transmission through perforated plates at high amplitude. *Journal of the Acoustical Society of America*, 79:942–951, 1986.

[7] T. Elnady and H. Boden. On semi-empirical liner impedance modeling with grazing flow. *AIAA*, pages 1–11, 2003.

[8] U. Ingård. Nonlinear distortion of sound transmitted through an orifice. *The Journal of the Acoustical Society of America*, 48(1A):32–33, 1970.

[9] C.K.W. Tam and K.A. Kurbatskii. Microfluid dynamics and acoustics of resonant liners. *AIAA Journal*, 38:1331–1339, 2000.

[10] K.K. Ahuja C.K.W. Tam, K.A. Kurbatskii and R.J. Gaetajr. A numerical and experimental investigation of the dissipation mechanisms of resonant acoustic liners. *Journal of Sound and Vibration*, 245(3):545 – 557, 2001.

[11] U. Michel D. Bechert and E. Pfizenmarier. Experiments on the transmission of sound through jets. In *American Institute of Aeronautics and Astronautics, Aeroacoustics Conference, 4th, Atlanta*, 1977.

[12] M.S. Howe. On the theory of unsteady high reynolds number flow through a circular aperture. *Royal Society of London Proceedings A*, 366:205–233, 1979.

[13] M.S. Howe. The dissipation of sound at an edge. *Journal of Sound and Vibration*, 70:407–411, 1980.

[14] M.S. Howe. *Acoustics of Fluid-structure interactions*. Cambridge University Press, 1998.

[15] I. J. Hughes and A. P. Dowling. The absorption of sound by perforated linings. *Journal of Fluid Mechanics*, 218:299–335, 1990.

[16] J. D. Eldredge and A.P. Dowling. The absorption of axial acoustic waves by a perforated liner with bias flow. *Journal of Fluid Mechanics*, 485:307–335, 2003.

[17] D. Ronneberger. The acoustical impedance of holes in the wall of flow ducts. *Journal of Sound and Vibration*, 24:133–150, 1972.

[18] T. Luong, M.S. Howe, and R.S. McGowan. On the rayleigh conductivity of a bias-flow aperture. *Journal of Fluids and Structures*, 21(8):769 – 778, 2005.

[19] J. Carrotte J. Rupp and A. Spencer. Interaction between the acoustic pressure fluctuations and the unsteady flow field through circular holes. *Journal of Engineering for Gas Turbines and Power*, 132(6):061501, 2010.

[20] P. Testud, Yves Aurégan, P Moussou, and Avraham Hirschberg. The whistling potentiality of an orifice in a confined flow using an energetic criterion. *Journal of Sound and Vibration*, 325(4):769–780, 2009.

[21] E. Dokumaci. A note on transmission of sound in a wide pipe with mean flow and viscothermal attenuation. *Journal of sound and vibration*, 208(4):653–655, 1997.

[22] Y. Aurégan and R. Starobinski. Determination of acoustical energy dissipation/production potentiality from the acoustical transfer functions of a multiport. *Acta Acustica united with Acustica*, 85(6):788–792, 1999.

[23] A. Cummings and W. Eversman. High amplitude acoustic transmission through duct terminations: Theory. *Journal of Sound and Vibration*, 91(4):503–518, 1983.